Experimental determination of the lidar overlap profile with Raman lidar

Ulla Wandinger and Albert Ansmann

The range-dependent overlap between the laser beam and the receiver field of view of a lidar can be determined experimentally if a pure molecular backscatter signal is measured in addition to the usually observed elastic backscatter signal, which consists of a molecular component and a particle component. Two methods, the direct determination of the overlap profile and an iterative approach, are presented and applied to a lidar measurement. The measured overlap profile accounts for actual system alignment and for all system parameters that are not explicitly known, such as actual laser beam divergence and spatial intensity distribution of the laser light. © 2002 Optical Society of America

OCIS codes: 010.0010, 010.3640, 120.0120, 120.0280, 280.0280, 280.3640.

1. Introduction

The incomplete overlap between the laser beam and the receiver field of view significantly affects lidar observations of particle optical properties in the near-field range. The effect can considerably influence vertical profiling up to several kilometers in the case of coaxial systems with a narrow receiver field of view of less than 0.5 mrad. Without correction of the range-dependent overlap characteristics, a proper study of the important exchange processes of anthropogenic pollution between the sources and the lower-most layers of the troposphere is not possible.

Several attempts have been made to determine the profile of the overlap factor (also denoted as geometric form factor or crossover function in the literature) analytically, 1-3 by the application of a ray-tracing model, 4 or experimentally. 5-7 For theoretical approaches, a good understanding of the actual light distribution in the laser beam cross section, the beam divergence, the beam direction, and the characteristics of the receiver unit (telescope optics, detector channel performance) is needed to obtain an overlap profile with sufficient accuracy. Our experience shows that this information is generally not available, especially during field campaigns. For the proposed

Here we present a simple technique for determination of the overlap function, which is based on the measurement of a pure molecular (nitrogen or oxygen Raman) backscatter signal in addition to the elastic backscatter signal performed with an aerosol Raman lidar.8,9 The method works without the need to know the above-mentioned lidar system parameters and under homogeneous as well as inhomogeneous aerosol conditions. The basic assumption is that the overlap profiles for both the elastic backscatter and the Raman channels are identical. The only input data set that can influence the result significantly is the profile of the particle extinction-to-backscatter ratio (lidar ratio). The lidar ratio effect is minimized in cases with clear atmospheric conditions. In principle, a high-spectral-resolution lidar¹⁰ that measures the aerosol signal and the respective Rayleigh signal separately can also be used to determine the overlap according to our method.

2. Method

The lidar equations for the aerosol (elastic backscatter) and the Raman backscatter signals can be written as

$$P_0(z) = C_0 O_0(z) z^{-2} [\beta_{0,P}(z) + \beta_{0,M}(z)] T_0(z)^2, \quad (1)$$

$$P_{R}(z) = C_{R}O_{R}(z)z^{-2}\beta_{R}(z)T_{0}(z)T_{R}(z), \qquad (2)$$

experimental attempts, a trustworthy determination is possible under homogeneous aerosol conditions only. All the methods use the elastic backscatter signal and must assume range-independent backscattering and light extinction in the near field, which often does not hold in the lowermost troposphere.

U. Wandinger (ulla@tropos.de) and A. Ansmann (albert@tropos.de) are with the Institute for Tropospheric Research, Permoserstrasse 15, Leipzig 04318, Germany.

Received 13 December 2000; revised manuscript received 22 June 2001.

^{0003-6935/02/030511-04\$15.00/0}

^{© 2002} Optical Society of America

where P is the received power; 0 and R represent the laser wavelength λ_0 and the Raman wavelength λ_R , respectively; C_0 and C_R are the system constants for the elastic and molecular channels, respectively; and O(z) denotes the overlap factor. O(z) is zero at the lidar (no overlap) and typically reaches 1 (complete overlap) for large distances. $O_0(z) = O_R(z)$ is assumed in our approach. As our experience shows, this assumption is sufficiently valid for a well-aligned interference-filter polychromator with approximately equal optical path lengths between the telescope and the photomultiplier for both wavelengths. In Eq. (1), $\beta_{0,P}$ and $\beta_{0,M}$ represent the elastic backscatter coefficients of particles and molecules at λ_0 , respectively, and β_R in Eq. (2) is the nitrogen or oxygen Raman backscatter coefficient at λ_R . T_0 describes the atmospheric transmission at λ_0 between the lidar and the backscatter region, and T_R is the atmospheric transmission at λ_R along the way back to the lidar after Raman scattering.

The overlap profile can be determined either directly or iteratively. By rearranging Eq. (2), we obtained $O(z) = O_R(z)$ directly from the measured signal $P_R(z)$, according to

$$O(z) = \frac{P_{R}(z)z^{2}}{C_{R}\beta_{R}(z)T_{0}(z)T_{R}(z)},$$
 (3)

after correction of the range dependence of the molecular signal (z^2) , after correction of the molecular and particle transmission contributions to T_0 and T_R , and after accounting for the air-density decrease, which determines the change of $\beta_R(z)$ with range z. The nitrogen or oxygen Raman backscatter cross section (per molecule) is range independent. The unknown constant C_R was finally selected such that the maximum values of the corrected, noisy signal profile varied around 1. These maximum values are usually found in the far-field range for a well-adjusted lidar.

The air-density decrease and the molecular transmission properties can be calculated with sufficient accuracy from model temperature and pressure profiles or respective data of a nearby radiosonde ascent. The particle transmission properties are estimated from the particle backscatter-coefficient profile that was obtained from the profile of the signal ratio of the aerosol signal [Eq. (1)] to the molecular signal [Eq. (2)] by application of the Raman lidar method.9 Since the calculation is based on signal ratios and $O_0(z) = O_R(z)$ is assumed, the solution is not affected by the overlap effect. To calculate the contribution of particle extinction to the atmospheric transmission, the backscatter-coefficient profile must be converted into a particle extinction-coefficient profile by means of an assumed profile of the extinction-tobackscatter ratio (lidar ratio). A good guess of the lidar ratio in the near-field range is often available from the (same) Raman lidar measurement at greater distances. However, to avoid considerable uncertainties caused by the lidar ratio estimates, lidar measurements performed under clear conditions (particle transmission >0.9) are preferable for determination of the overlap profile.

The iterative approach makes use of the fact that the deviation between the Klett solution, 11 $\beta_{\rm Klett}(z),$ for the backscatter coefficient, which is calculated from the elastic backscatter signal, and the Raman lidar solution, $\beta_{\rm Raman}(z),$ contains information about the incomplete overlap. Here, the lidar-ratio profile is needed as input for the Klett procedure. This iterative method is of practical use because computer codes for the determination of $\beta_{\rm Klett}(z)$ and $\beta_{\rm Raman}(z)$ are usually available if elastic backscatter and Raman signals are measured. Thus, the computation of Eq. (3) and of the terms in Eq. (3) is not necessary to obtain the overlap profile.

The basic idea behind the iterative approach is that the aerosol signal, after correction of the range and overlap dependencies, is proportional to the total backscatter coefficient [see Eq. (1)]:

$$P_0(z)O(z)^{-1}z^2 \propto \beta_{\text{Raman}}(z) + \beta_{0,M}(z),$$
 (4)

with $\beta_{0,P}(z) = \beta_{\text{Raman}}(z)$, whereas the aerosol signal, corrected for the range dependence only, is mainly a function of the combined effect of total backscattering and the range-dependent overlap. This dependency is expressed by means of the Klett solution,

$$P_0(z)z^2 \propto \beta_{\text{Klett}}(z) + \beta_{0,M}(z). \tag{5}$$

The relative difference between the Klett and the Raman lidar solutions [see relations (4) and (5)],

$$\frac{\beta_{\text{Raman}}(z) - \beta_{\text{Klett}}(z)}{\beta_{\text{Raman}}(z) + \beta_{0,M}(z)} \propto \frac{P_0(z)O(z)^{-1}z^2 - P_0(z)z^2}{P_0(z)O(z)^{-1}z^2}$$

$$\propto 1 - O(z). \tag{6}$$

is used in the following to reduce the overlap effect on the aerosol signal iteratively.

In the first step (i = 1) the Klett method is applied to the uncorrected elastic backscatter signal. $\beta_{\text{Klett},i=1}(z)$ is used to solve the expression

$$\Delta O_i(z) = \frac{\beta_{\text{Raman}}(z) - \beta_{\text{Klett},i}(z)}{\beta_{\text{Raman}}(z) + \beta_{0,M}(z)}.$$
 (7)

With $\Delta O_1(z)$ the elastic backscatter signals are corrected as follows:

$$P_{0i+1}(z) = P_{0i}(z)[1 + \Delta O_i(z)]. \tag{8}$$

By reapplying the Klett method (step i=2), now to the improved signal profile $P_{0,2}(z)$, we obtained an improved backscatter coefficient profile $\beta_{\mathrm{Klett},2}(z)$. After inserting $\beta_{\mathrm{Klett},2}(z)$ into Eq. (7) and $\Delta O_2(z)$ into Eq. (8) we further corrected the signal profile for the overlap effect. Approximately 10–12 iterations are sufficient to remove the overlap effect completely as shown by our simulations. By comparing the measured signal profile with the corrected signal profile

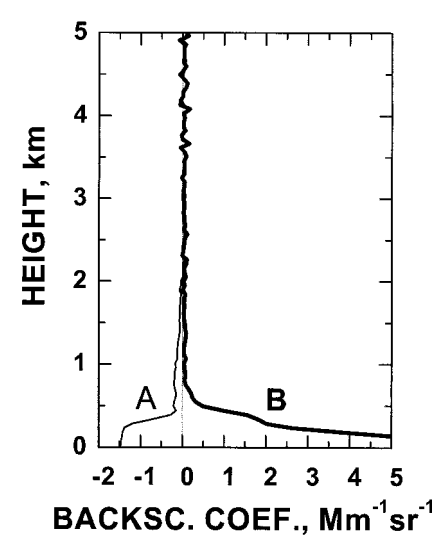


Fig. 1. Klett solution (curve A, overlap effect is ignored) and Raman lidar solution (curve B) for the particle backscatter coefficient. The lidar observation was in clean, maritime air. For the Klett procedure we assumed a lidar ratio of 25 sr, which is typical for maritime aerosols.

we obtained the overlap profile. This profile is identical to the one determined directly with Eq. (3).

3. Experiment

Figure 1 shows an observation of the 532-nm particle backscatter coefficient obtained by use of the Raman lidar method (532-nm laser wavelength, 607-nm nitrogen Raman wavelength) together with the Klett solution calculated from the uncorrected 532-nm signal. The comparison of the two profiles clearly shows the overlap effect. The measurement was performed in a clean marine environment on the Portuguese coast. A coaxial lidar system¹² with a laser beam divergence of approximately 0.1 mrad and a receiver field of view of approximately 0.3 mrad was used. The lidar pointed to a zenith angle of 60°. The backscatter profile indicates the marine boundary layer with a top height of 500 m. The troposphere above 500-m height was almost aerosol free. The particle optical depth and the particle transmission were approximately 0.08 and 0.92, respectively, at 532-nm wavelength.

Figure 2 presents the corresponding overlap profile determined from Eq. (3). A typical lidar ratio for maritime particles of 25 sr is assumed in the estimation of the particle transmission [see Eq. (3)]. The Klett solution, β_{Klett} , is equal to the Raman lidar solution, β_{Raman} , in Fig. 1, if the overlap profile in Fig. 2 is applied to the measured aerosol backscatter signal.

The consequence of overlap correction in the determination of the particle extinction-coefficient profile is demonstrated in Fig. 3. The extinction coefficient was calculated with the Raman lidar method.⁹ The overlap function in Fig. 2, which was observed on 26 June 1997, was applied to a lidar measurement that

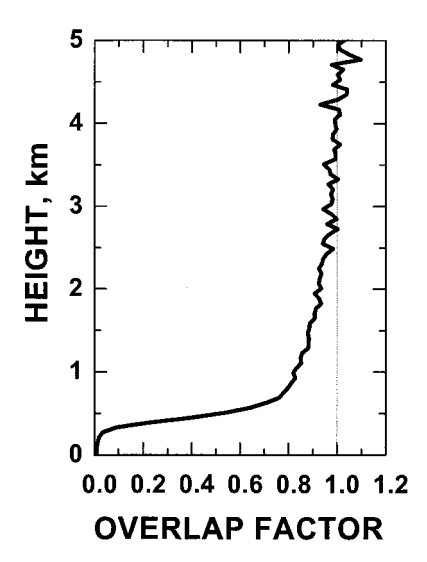


Fig. 2. Overlap profile that we determined by applying the direct method [Eq. (3)].

was performed several weeks later on 18 July 1997 at a zenith angle of 60°. On that day, a layer with continental particles was present above the marine boundary layer. $^{13}\,$ In the data analysis, the Raman lidar signal was first divided by the overlap factor. Then the corrected molecular signal profile was smoothed with vertical window lengths of 300 m (<1200-m height), 600 m (1200-2400-m height), and 1200 m (>2400-m height). From this smoothed signal profile we calculated the extinction values.

Figure 3 clearly shows the importance of the overlap correction. As can be seen, the measurements are useless for heights below approximately 1500 m if the overlap effect is ignored. It would not be possible to investigate the interaction between the marine

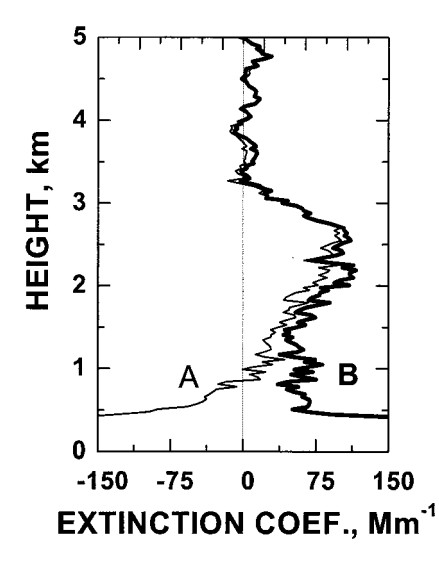


Fig. 3. Particle extinction coefficient determined from the nitrogen Raman signal profile when we ignored the incomplete overlap (curve A) and when we considered the overlap profile (shown in Fig. 2) in the data analysis (curve B).

boundary layer and the continental plume in terms of the extinction profile.

The method presented here has been extensively tested and successfully applied to experimental data obtained during several international aerosol field campaigns in Europe^{13,14} and Asia.^{15–17} However, problems often occurred at distances of <1000 m. which is mainly caused by the fact that the actual overlap characteristics differ slightly from those that are assumed in the data analysis and that were determined several days or weeks before or after the actual observation. This effect has the most influence on the results at the shortest distances (lowest heights). Furthermore, errors in the overlap profile determination caused by the basic assumption of the method (identical overlap profiles for both receiver channels) cannot be excluded, although comparisons with airborne lidar observations of the backscatter profile indicated proper alignment of the two channels. Good agreement was also found between starphotometer observations of the optical depth and the lidar-derived optical depth based on the columnintegrated backscatter coefficients,13 which underlines the reliability of the Raman lidar solutions for the backscatter coefficient and thus the proper alignment of the system. Finally, the input-lidar ratio profile can also lead to uncertainties that affect the extinction profiling in the near-field range.

References

- T. Halldórsson and J. Langerholc, "Geometrical form factors for the lidar function," Appl. Opt. 17, 240-244 (1978).
- 2. K. Sassen and G. C. Dodd, "Lidar crossover function and misalignment effects," Appl. Opt. 21, 3162–3165 (1982).
- 3. G. M. Ancellet, M. J. Kavaya, R. T. Menzies, and A. M. Brothers, "Lidar telescope overlap function and effects of misalignment for unstable resonator transmitter and coherent receiver," Appl. Opt. 25, 2886–2890 (1986).
- R. Velotta, B. Bartoli, R. Capobianco, and N. Spinelli, "Analysis of the receiver response in lidar measurements," Appl. Opt. 37, 6999-7007 (1998).
- Y. Sasano, H. Shimizu, N. Takeuchi, and M. Okuda, "Geometrical form factor in the laser radar equation: an experimental determination," Appl. Opt. 18, 3908–3910 (1979).
- 6. K. Tomine, C. Hirayama, K. Michimoto, and N. Takeuchi, "Experimental determination of the crossover function in the

- laser radar equation for days with a light mist," Appl. Opt. 28, 2194–2195 (1989).
- S. W. Dho, Y. J. Park, and H. J. Kong, "Experimental determination of a geometrical form factor in a lidar equation for an inhomogeneous atmosphere," Appl. Opt. 36, 6009-6010 (1997).
- 8. D. N. Whiteman, S. H. Melfi, and R. A. Ferrare, "Raman lidar system for the measurement of water vapor and aerosols in the Earth's atmosphere," Appl. Opt. **31**, 3068–3082 (1992).
- A. Ansmann, U. Wandinger, M. Riebesell, C. Weitkamp, and W. Michaelis, "Independent measurement of extinction and backscatter profiles in cirrus clouds by using a combined Raman elastic-backscatter lidar," Appl. Opt. 31, 7113–7131 (1992).
- 10. C. J. Grund and E. W. Eloranta, "The University of Wisconsin high spectral resolution lidar," Opt. Eng. **30**, 6–12 (1991).
- 11. F. G. Fernald, "Analysis of atmospheric lidar observations: some comments," Appl. Opt. 23, 652-653 (1984).
- D. Althausen, D. Müller, A. Ansmann, U. Wandinger, H. Hube,
 E. Clauder, and S. Zörner, "Scanning six-wavelength elevenchannel aerosol lidar," J. Atmos. Oceanic Technol. 17, 1469– 1482 (2000).
- A. Ansmann, F. Wagner, D. Althausen, D. Müller, A. Herber, and U. Wandinger, "European pollution outbreaks during ACE 2: Lofted aerosol plumes observed with Raman lidar at the Portuguese Coast," J. Geophys. Res. 106, 20725–20733 (2001).
- 14. U. Wandinger, D. Müller, C. Böckmann, D. Althausen, V. Matthias, J. Bösenberg, V. Weiss, M. Fiebig, M. Wendisch, A. Stohl, and A. Ansmann, "Optical and microphysical characterization of biomass-burning and industrial-pollution aerosols from multiwavelength lidar and aircraft measurements," J. Geophys. Res. (to be published).
- A. Ansmann, D. Althausen, U. Wandinger, K. Franke, D. Müller, F. Wagner, and J. Heintzenberg, "Vertical profiling of the Indian aerosol plume with six-wavelength lidar during INDOEX: A first case study," Geophys. Res. Lett. 27, 963–966 (2000).
- D. Müller, K. Franke, F. Wagner, D. Althausen, A. Ansmann, and J. Heintzenberg, "Vertical profiling of optical and physical particle properties over the tropical Indian Ocean with sixwavelength lidar. 1. Seasonal cycle," J. Geophys. Res. 106, 28567–28576 (2001).
- D. Müller, K. Franke, F. Wagner, D. Althausen, A. Ansmann,
 J. Heintzenberg, and G. Verver, "Vertical profiling of optical and physical particle properties over the tropical Indian Ocean with six-wavelength lidar. 2. Case studies," J. Geophys. Res. 106, 28577–28596 (2001).